RAPID COMMUNICATIONS

PHYSICAL REVIEW B VOLUME 43, NUMBER 16 1 JUNE 1991

# Chirality selection by magnetoelectric coupling in frustrated hexagonal antiferromagnets

M. L. Plumer
*Centre de Recherche en Physique du Solide et Département de Physique, Université de Sherbrooke, Sherbrooke, Québec, Canada J1K 2R1*

H. Kawamura
*Department of Physics, College of General Education, Osaka University, Toyonaka, Osaka 560, Japan*

A. Caillé
*Centre de Recherche en Physique du Solide et Département de Physique, Université de Sherbrooke, Sherbrooke, Québec, Canada J1K 2R1*

(Received 15 January 1991)

Symmetry arguments are used to demonstrate that an electric field applied in the basal plane of a stacked triangular antiferromagnet breaks chiral degeneracy associated with the frustration-induced 120° spin structure. This is achieved through magnetoelectric coupling which introduces a Dzyaloshinsky-Moryia type of interaction. The electric-field–temperature phase diagram is investigated through the analysis of a Landau-type free energy and the connection with recent renormalization-group calculations is made. Possible applications to $CsMnBr_3$ and related materials are discussed.

It is known that the chirality of helically polarized magnetic structures in crystals that do not contain a center of inversion symmetry is determined by the sign of the antisymmetric Dzyaloshinsky-Moriya (DM) exchange interaction.[1–3] In materials which do have a center of inversion, however, right- and left-handed helical states are energetically equivalent. Such chiral degeneracy occurs in the stacked triangular (hexagonal) lattice with near-neighbor antiferromagnetic bonds where tripartite frustration stabilizes the so-called 120° spin structure. In the case of planar anisotropy, this helicity degree of freedom gives rise to an Ising-like ($Z_2$) discrete degeneracy[4] addition to the usual $XY$ ($S_1$) continuous degeneracy so that the order parameter is characterized by $V=Z_2xS_1$. One of us[5,6] has recently demonstrated that this symmetry is responsible for a new ($n=2$) chiral universality class.[7] The critical properties of such systems have been further illuminated by considering the effects of an applied in-plane magnetic field. Tetracritical behavior, as observed[8] in the quasi-one-dimensional hexagonal insulator $CsMnBr_3$, is now well understood.[9,10]

The general phenomenon known as the *magnetoelectric effect*[11] usually refers to the appearance of a magnetic (electric) moment in response to an applied electric (magnetic) field. Magnetoelectric coupling can, however, cause a variety of other effects.[12] Over ten years ago, the results of a remarkable experiment on $ZnCr_2Se_4$ were reported,[13] which established that the sense of chirality in certain helimagnets can be controlled. A crystal of this tetragonal (below $T_N$) semiconductor was cooled in the presence of both electric and magnetic fields. Spin-flip neutron diffraction measurements determined that a conical magnetic structure of definite helicity was produced.

The present study was motivated by the observations in this earlier work and by the continuing interest in the critical behavior of frustrated antiferromagnets. Symmetry arguments are used here to construct the lowest-order coupling between the spin vector **S** and electric-field (**E**) induced polarization vector **P** in the case where the magnetic ions of an insulator occupy the sites of a simple hexagonal lattice with planar anisotropy. The overall crystal structure is assumed to contain a center of inversion symmetry. The result of this analysis is a magnetoelectric coupling term with a form identical to the usual DM interaction. With **E** in the basal plane, the effect of this interaction is to stabilize incommensurate magnetic ordering. This takes the form of a slightly distorted 120° spin structure in the case where the nearest-neighbor exchange interactions are antiferromagnetic. It is further demonstrated that chiral degeneracy is removed if the field is applied perpendicular to a crystallographic basal-plane axis. A model Landau free energy serves as the basis for an investigation of the electric-field–temperature phase diagram within a mean-field approximation. Numerical results are presented which indicate the possibility of (at least) two distinct types of multicritical point behavior, depending on the relative magnitudes of certain parameter values. These results are relevant to the recent renormalization-group calculations of Ref. 5 and suggest that the experimental study of critical fluctuation effects associated with crossover behavior between $n=2$ chiral and $XY$ universality classes is feasible.

Construction of terms which contribute to the magnetic Hamiltonian (or free energy) must satisfy time-reversal symmetry (only even powers of **S** can occur) and must be invariant with respect to the symmetry operations of the crystal space group.[14,15] Of interest here are terms linear in **P** and quadratic in **S**. In the case of hexagonal crystals with a center of inversion symmetry, the only such term to occur can be expressed as[16]

$$\mathcal{H}_C = 1/(2V)\int d\mathbf{r}\,d\mathbf{r}'\,C(\boldsymbol{\tau})(\mathbf{P}\times\boldsymbol{\tau})_z\cdot[\mathbf{s}(\mathbf{r})\times\mathbf{s}(\mathbf{r}')]\,, \qquad (1)$$

 

where $\tau=\mathbf{r}-\mathbf{r}'$, $C(-\tau)=C(\tau)$, and the subscript $z$ indicates $\hat{\mathbf{z}}$ component. [We adopt here a perpendicular coordinate system $(\hat{\mathbf{x}},\hat{\mathbf{y}},\hat{\mathbf{z}})$, with $\hat{\mathbf{z}}$ along the hexagonal $c$ axis and $\hat{\mathbf{x}}$ along a basal-plane $a$ axis.] The polarization vector $\mathbf{P}$ is assumed to be proportional to the applied field $\mathbf{E}$. This is precisely of the form often written for the DM interaction, $\mathbf{D}\cdot\mathbf{S}_i\times\mathbf{S}_j$.

For the purpose of evaluating ground-state and equilibrium magnetic properties, it is convenient to adopt our previous representation of the spin density:[10,15]

$$\mathbf{s}(\mathbf{r})=(V/N)\sum_{\mathbf{R}}\rho(\mathbf{r})\delta(\mathbf{r}-\mathbf{R}), \tag{2}$$

where $\mathbf{R}$ denotes hexagonal lattice sites and $\rho$ characterizes the long-range magnetic order,

$$\rho(\mathbf{r})=\mathbf{S}e^{i\mathbf{Q}\cdot\mathbf{r}}+\mathbf{S}^*e^{-i\mathbf{Q}\cdot\mathbf{r}}, \tag{3}$$

and $\mathbf{S}=\mathbf{S}_1+i\mathbf{S}_2$, with $\mathbf{S}_1$ and $\mathbf{S}_2$ being real vectors. With only nearest-neighbor interactions included, the magnetoelectric coupling contribution to the ground-state energy is given by

$$E_C=i\tilde{C}_{\mathbf{Q}}P\hat{\mathbf{z}}\cdot(\mathbf{S}\times\mathbf{S}^*), \tag{4}$$

where

$$\tilde{C}_{\mathbf{Q}}=2C_\perp[2bp_x\cos\tfrac{1}{2}q_x\sin q_y - ap_y(\sin q_x+\sin\tfrac{1}{2}q_x\cos q_y)], \tag{5}$$

$C_\perp=(V/N)C(\mathbf{a})$, $\mathbf{P}=P(p_x\hat{\mathbf{x}}+p_y\hat{\mathbf{y}})$, $q_x=aQ_x$, $q_y=bQ_y$, and $b=(\sqrt{3}/2)a$. Interactions of this type favor a spin density with helical polarization,[1,2] e.g.,

$$\mathbf{S}_1=(S/\sqrt{2})\hat{\mathbf{x}},\quad \mathbf{S}_2=(S/\sqrt{2})\hat{\mathbf{y}}. \tag{6}$$

Magnetic exchange interactions are assumed to have the usual form

$$\mathcal{H}_J=(1/2V)\int d\mathbf{r}\,d\mathbf{r}'J(\tau)\mathbf{s}(\mathbf{r})\cdot\mathbf{s}(\mathbf{r}') \tag{7}$$

and contribute to the ground-state energy[10] $E_J=J_{\mathbf{Q}}\mathbf{S}\cdot\mathbf{S}^*$ where, with near-neighbor interactions only,[15]

$$J_{\mathbf{Q}}=2J_\parallel\cos(q_z)+2J_\perp[\cos(q_x)+2\cos(\tfrac{1}{2}q_x)\cos(q_y)], \tag{8}$$

and both $J_\parallel=(V/N)J(\mathbf{c})$ and $J_\perp=(V/N)J(\mathbf{a})$ are assumed here to be positive (although the sign of $J_\parallel$ is not relevant to the principal results of interest discussed below). Modulation of the spin density determined by the antiferromagnetic interactions (8) yields a period-2 structure along the $c$ axis and a period-3 ordering in the basal plane, $\mathbf{Q}_n=(4\pi/3a)\hat{\mathbf{a}}_n+(\pi/c)\hat{\mathbf{c}}$ where $\hat{\mathbf{a}}_n$ indicates one of the six basal-plane crytallographic directions. With helical polarization of the form (6), the 120° spin structure is realized where positive chirality states $\mathbf{Q}_\perp=+(4\pi/3a)\hat{\mathbf{x}}$, $-(2\pi/3a)\hat{\mathbf{x}}\pm(\pi/b)\hat{\mathbf{y}}$, and negative chirality states $\mathbf{Q}_\perp=-(4\pi/3a)\hat{\mathbf{x}}$, $+(2\pi/3a)\hat{\mathbf{x}}\pm(\pi/b)\hat{\mathbf{y}}$ are energetically equivalent. Note that $\mathbf{S}$ and the relevant modulation $\mathbf{Q}_\perp$ both lie in the same (basal) plane, which differs from the usual helical ordering where $\mathbf{S}$ and $\mathbf{Q}$ are perpendicular. Chirality $\kappa$ is defined here by the expression[5]

$$\kappa=(1/N)\sum_i\kappa_i,\quad \kappa_i=2/(\sqrt{3}S^2)(s_i^xs_{i+1}^y-s_i^ys_{i+1}^x), \tag{9}$$

where $i$ labels sites along a direction $\hat{\mathbf{a}}_n$.

Consider now the effects of magnetoelectric coupling (4) on the magnetic wave vector $\mathbf{Q}$, determined by minimization of the energy $E_Q=(J_{\mathbf{Q}}+P\tilde{C}_{\mathbf{Q}})S^2$. Since $\tilde{C}_{\mathbf{Q}}$ is zero for the 120° spin structure, this commensurate state is destabilized in favor of an incommensurate ordering. The two configurations $\mathbf{P}\parallel\hat{\mathbf{x}}$ and $\mathbf{P}\parallel\hat{\mathbf{y}}$ (i.e., parallel and perpendicular to an $\hat{\mathbf{a}}_n$ axis, respectively) are considered and results are given only for the cases where, in the limit $P\to 0$, $\mathbf{Q}_\perp=\pm(4\pi/3a)\hat{\mathbf{x}}$ (since the other four wave vectors give equivalent structures). For $\mathbf{P}\parallel\hat{\mathbf{x}}$, $\tilde{C}_{\mathbf{q}}$ is an even function of $q_x$ and no chirality selection occurs. The equilibrium magnetic wave vector for small magnetoelectric coupling is given by $q_x\cong\pm[4\pi/3+(1\sqrt{3})\delta_b^2]$ and $q_y\cong\delta_b$ where $\delta_b=bPC_\perp/J_\perp$. With $\mathbf{P}\parallel\hat{\mathbf{y}}$, however, $\tilde{C}_{\mathbf{q}}$ is an odd function of $q_x$ and *chiral symmetry is broken.* It can be seen from the plot of $E_q$ shown in Fig. 1 that a positive helicity state ($q_x\cong+4\pi/3$) is stabilized for $C_\perp>0$ and that a negative helicity state ($q_x\cong-4\pi/3$) occurs for $C_\perp<0$ (c.f. Fig. 2 of Ref. 2). For $C_\perp>0$, the minimum in $E_q$ occurs at $q_x\cong4\pi/3-\delta_a$, where $\delta_a=aPC_\perp/J_\perp$, and $q_y=0$, with the magnetoelectric coupling energy given by $E_C\cong-\frac{3}{2}C_\perp aP(\delta_a+\sqrt{3}\delta_a^2/4)S^2$. The other local minimum seen in Fig. 1 for this case occurs at $q'_x\cong-4\pi/3-\delta_a$ with a higher energy by an amount $+\frac{3}{4}C_\perp aP\sqrt{3}\delta_a^2S^2$.

Formulation of a Landau-type free energy for the purpose of investigating the electric-field–temperature phase diagram follows from general principles outlined in our earlier work.[9,10] The result, to low order, can be expressed as

$$F=A_{\mathbf{Q}}S^2+\tfrac{1}{2}A_EP^2+iC_{\mathbf{Q}}P\hat{\mathbf{z}}\cdot(\mathbf{S}\times\mathbf{S}^*)+B_1S^4 + \tfrac{1}{2}B_2|\mathbf{S}\cdot\mathbf{S}|^2+2\tilde{B}_4|\mathbf{P}\cdot\mathbf{S}|^2+\tilde{B}_5P^2S^2-\mathbf{P}\cdot\mathbf{E}, \tag{10}$$

where $A_{\mathbf{Q}}=aT+J_{\mathbf{Q}}$ and the parameters $\{a, J_\parallel, J_\perp, A_E, C_\perp, B_1, B_2, \tilde{B}_4, \tilde{B}_5\}$ are specific to the material of interest. Except for the DM interaction term, this free energy has a

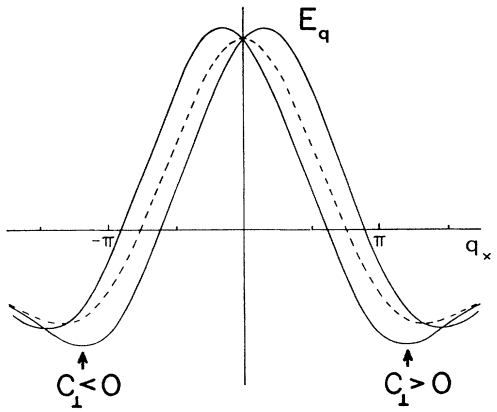


FIG. 1. Wave-vector dependence of the ground-state energy. Broken curve shows chirality-degenerate minima at $q_x=\pm4\pi/3$ resulting from antiferromagnetic exchange. Solid curves show minima (arrows) at $q_x\cong+4\pi/3$ (positive chirality) for $C_\perp>0$ and at $q_x\cong-4\pi/3$ (negative chirality) for $C_\perp<0$ as a result of the inclusion of the magnetoelectric coupling term (4).

structure similar to the one used by us to study the effects of an applied magnetic field on the frustrated hexagonal lattice. A positive coefficient $B_2$ serves to stabilize the helical polarization of the spin density in the absence of any external fields. The coupling term $\tilde{B}_4$ favors a configuration $\mathbf{S}\perp\mathbf{P}$ (with $\tilde{B}_4>0$), i.e., a linearly polarized state. The result of this competition is an elliptical polarization. In contrast with the magnetic field case, however, the $\tilde{B}_4$ term must be relatively large to realize a complete linear polarization since the DM term above (also of order $S^2$) favors the helical state. Note that in this case, the DM term would be zero so that commensurate ordering, as at $E=0$, occurs.

Schematics of the two types of phase diagrams obtained from numerical minimization of $F$ with $\mathbf{E}\parallel\pm\hat{\mathbf{y}}$ are depicted in Fig. 2. The parameters $a$, $A_E$, $B_1$, and $B_2$ were each set to unity and various combinations of relative magnitudes for $J_\parallel$, $J_\perp$, $C_\perp$, and $\tilde{B}_4$, all taken to be positive, were considered. Results as shown in Fig. 2(a) were found for cases where $\tilde{B}_4$ was not large compared with $C_\perp$. A relatively strong interaction $|\mathbf{P}\cdot\mathbf{S}|^2$ stabilizes the linear (commensurate) phase as shown in Fig. 2(b). The ordered states can be further characterized by the chirality (9), where $|\kappa|=1$, $|\kappa|<1$, and $\kappa=0$ correspond to helical, elliptical, and linear phases, respectively. Note that the $E=0$ axis, where the helical-commensurate phase occurs, is a line where incommensurability vanishes continuously and chirality jumps from $-1$ to $+1$ with increasing electric-field strength.

Cooling a stacked triangular antiferromagnet in an electric field combined with polarized neutron scattering[13] may enable experimental measurement of the chirality associated with the "helical" spin ordering. In the absence of the chiral-symmetry breaking field, the ordered state of these materials is spatially divided into chiral domains with right- and left-handed helicities of equal population.[17] In such cases, neutron-polarization effects arising from chirality would average to zero. However, the magnetoelectric cooling technique may be used to prepare a single-chiral-domain ordered state. Polarized neutron analysis then becomes useful. The purely magnetic elastic cross section of neutrons with incident polarization $\mathcal{P}$ can be expressed schematically as[18]

$$d\sigma/d\Omega \propto \langle \mathbf{S}_\perp(\mathbf{q})\cdot\mathbf{S}_\perp(-\mathbf{q})\rangle + i\mathcal{P}\cdot\langle \mathbf{S}_\perp(\mathbf{q})\times\mathbf{S}_\perp(-\mathbf{q})\rangle , \tag{11}$$

where $\mathbf{q}$ is the scattering vector and $\mathbf{S}_\perp=\hat{\mathbf{q}}x(\mathbf{S}x\hat{\mathbf{q}})$. The total chirality $\bar{\kappa}$ can be expressed as

$$\bar{\kappa}\propto i\int d\mathbf{q}[\mathbf{S}(\mathbf{q})\times\mathbf{S}(-\mathbf{q})]_z , \tag{12}$$

where integration over $\mathbf{q}$ is taken around a Bragg point $\mathbf{Q}$ (see Appendix C of Ref. 5). This expression is just the second term of (11) integrated over $\mathbf{q}$ and, in principle, may be determined experimentally by either of the following two methods: by measuring the difference between the scattering intensities from the up $(+\mathcal{P})$ and down $(-\mathcal{P})$ incident neutrons around a fixed point $\mathbf{Q}$, or by measuring the difference between the scattering intensities around the two distinct Bragg points $+\mathbf{Q}$ and $-\mathbf{Q}$ for a fixed polarization of incident neutrons. Note that the total chirality is related to the *integrated* intensity,[5] while the Bragg intensities are proportional to the square of the sublattice magnetization (conventional order parameter) even for polarized neutrons. In principle, the chiral susceptibility is also measurable by investigating the response $d\bar{\kappa}/dE$. In order to observe the desired effect, an electric field of sufficient strength to overcome domain-wall energies would be required; this is difficult to estimate, even if the value of $C_\perp$ were known. An electric field of 2.5 kV/cm produced a 95% single-domain sample in the experiments of Ref. 13.

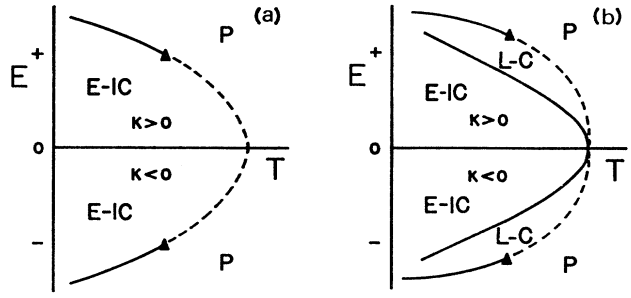


FIG. 2. Schematics of electric-field–temperature phase diagrams with $\mathbf{E}$ along $\hat{\mathbf{y}}$ and $C_\perp>0$ for the cases of a (a) small and (b) large coupling $\tilde{B}_4$ relative to $C_\perp$. Type (a) is found using, e.g., parameter values $J_\parallel=J_\perp=C_\perp=\tilde{B}_4=1$ and $J_\parallel=1$, $J_\perp=C_\perp=\tilde{B}_4=10^{-2}$, whereas type (b) results from using, e.g., $\tilde{B}_4=J_\parallel=1$, $J_\perp=C=10^{-2}$.

The results presented in this work are of particular interest in view of recent renormalization-group theory[5] and Monte Carlo simulations[6,19] of frustrated antiferromagnets. Chiral ordering takes place simultaneously with the helical spin order and is controlled by a new type of exponent, the chiral-crossover exponent $\phi_K$. It characterizes crossover effects between $XY$ universality (as predicted to occur with the DM term present) and $n=2$ chiral universality (with the DM term absent). Scaling arguments demonstrate that this exponent determines the behavior of the paramagnetic phase boundary [$E_C(T)$, as in Fig. 2(a)] close to the Néel temperature, $E_c^2\sim|T_N-T|^{\phi_K}$. Other chiral exponents of interest are $\beta_K$, characterizing the singular temperature dependence of the chirality (12), and $\gamma_K$ associated with the chiral susceptibility. The scaling relations $\phi_K=\beta_K+\gamma_K$ and $\alpha+2\beta_K+\gamma_K=2$ are expected to hold; indeed, recent Monte Carlo results[19] have given the estimates $\beta_K=0.44\pm0.04$, $\gamma_K=0.78\pm0.07$, $\phi_K=1.22\pm0.08$, and $\alpha=0.35\pm0.05$. Note that the predicted chirality exponent $\beta_K$ is slightly smaller than twice the order-parameter exponent $2\beta\cong0.52$ (Ref. 19) associated with the Bragg intensity. If, on the other hand, the transition is mean-field tricritical governed by the Gaussian fixed point (as suggested by the work of Ref. 7), the corresponding exponents should be $\beta_K=\frac{1}{2}$, $\gamma_K=\frac{1}{2}$, $\phi_K=1$, and $\alpha_K=\frac{1}{2}$.

In conclusion, it has been demonstrated that the helicity associated with frustrated triangular antiferromagnets

can be controlled by the application of an electric field. The present formulation provides a realistic mechanism for continuously varying the strength of the chiral-symmetry-breaking term examined recently by renormalization-group and Monte Carlo methods. Possible experimental tests (e.g., on $CsMnBr_3$ and related materials[6]) of these theoretical predictions by means of the electromagnetic cooling technique thus remain most interesting.

This work was supported by the Natural Sciences and Engineering Research Council of Canada and Fonds FCAR pour l'Aide et le Soutien à la Recherche du Gouvernement du Québec.

[1]O. Nakanishi *et al.*, Solid State Commun. **35**, 995 (1980).
[2]P. Bak and M. H. Jensen, J. Phys. C **13**, L881 (1980).
[3]G. Shirane *et al.*, Phys. Rev. B **28**, 6251 (1983).
[4]J. Villain, J. Phys. (Paris) **38**, 385 (1977).
[5]H. Kawamura, Phys. Rev. B **38**, 4916 (1988); **42**, 2610(E) (1990).
[6]H. Kawamura, J. Appl. Phys. **63**, 3086 (1988); J. Phys. Soc. Jpn. **58**, 584 (1989); **59**, 2305 (1990).
[7]An alternate point of view has recently been proposed: P. Azaria, B. Delamotte, and T. Jolicoeur, Phys. Rev. Lett. **64**, 3175 (1990).
[8]B. D. Gaulin *et al.*, Phys. Rev. Lett. **62**, 1380 (1989); T. E. Mason *et al.*, Phys. Rev. B **42**, 2715 (1990); T. Goto, T. Inami, and Y. Ajiro, J. Phys. Soc. Jpn. **59**, 2328 (1990); M. Poirier *et al.*, Physica B **165**, 171 (1990).
[9]M. L. Plumer and A. Caillé, Phys. Rev. B **41**, 2543 (1990); H. Kawamura, A. Caillé, and M. L. Plumer, *ibid.* **41**, 4416 (1990); T. E. Mason, M. F. Collins, and B. D. Gaulin, J. Appl. Phys. **67**, 5421 (1990).
[10]M. L. Plumer and A. Caillé, Phys. Rev. B **42**, 10 388 (1990).
[11]*Magnetoelectric Interaction Phenomena in Crystals,* edited by A. J. Freeman and H. Schmid (Gordon and Breach, New York, 1975).
[12]See, e.g., L. P. Gor'kov and A. V. Sokol, Pis'ma Zh. Eksp. Teor. Fiz. **45**, 239 (1987) [JETP Lett. **45**, 299 (1987)].
[13]K. Siratori *et al.*, J. Phys. Soc. Jpn. **48**, 1111 (1980).
[14]M. B. Walker, Phys. Rev. B **22**, 1338 (1980).
[15]M. L. Plumer and A. Caillé, Phys. Rev. B **37**, 7712 (1988).
[16]Also see H. Yatom and R. Englman, Phys. Rev. **188**, 793 (1969).
[17]J. Baruchel, S. B. Palmer, and M. Schlenker, J. Phys. (Paris) **42**, 1279 (1981).
[18]M. Blume, Phys. Rev. **130**, 1670 (1963); S. M. Lovesey, *Theory of Neutron Scattering from Condensed Matter* (Clarendon, Oxford, 1984).
[19]H. Kawamura (unpublished).